Dielectric Material Characterization of Traffic Objects in Automotive Radar Applications

Sevda Abadpour*, Mario Pauli*, Marius Kretschmann*, Hasan Iqbal†, Philip Aust‡and Thomas Zwick*
*Institute of Radio Frequency Engineering and Electronics (IHE)
Karlsruhe Institute of Technology (KIT), Karlsruhe, Germany
†ADC Automotive Distance Control Systems GmbH, Continental, Germany
‡Mercedes-Benz AG, Germany
Email: sevda.abadpour@kit.edu

***Abstract*—A safe and comprehensive experimental verification of automotive radars is a significant challenge in the development process of autonomous driving technology. This challenge is an inevitable part of testing, whether in simulation or conventional real-road testing. In order to rely on software-in-the-loop (SIL) modeling and simulation, the test environment have to be modeled as realistic as the real test environment. One step in more realistic test environment modeling is characterizing the electromagnetic properties of the environmental materials in automotive radar frequency bands. Therefore, studying the radar reflectivity and scattering of traffic objects is one of the critical tasks for more realistic test environment modeling. This paper demonstrates a free-space measurement setup for dielectric material characterization based on the measured scattering parameters. In this procedure, deterministic tests are conducted to investigate the scattering parameters of the different traffic materials and calculate the effective dielectric constant using Muller's algorithm as well as their angle-dependent backscattering properties.**

***Index Terms*—Automotive radar application, electromagnetic scattering, free-space method, material characterization, millimeter-wave measurements.**

I. Introduction

To address the accretive necessity for the validation and verification (V&V) process of autonomous driving technology, a reliable perception and understanding of the environment are crucial. Therefore, a set of camera, lidar and radar sensors are used in autonomous driving technology to fulfill the safety requirements. Among all sensors, automotive radar sensors play a vital role in providing high-robustness data from the environment, especially in adverse weather conditions.

Simulation methods and virtual validation test approaches, X-in-the-Loop (XiL), are in high demand for securing and homologating the functionality of automotive radar sensors [1]. Therefore, modeling traffic environments is important to approach realistic simulation results [2]. An essential prerequisite in rendering the simulation environment is to correctly define the material specification of different objects in the environment. It is due to the fact that the significant multipath propagation arises from electromagnetic (EM) wave reflections of various materials [3]. The reflection characteristics of materials depend on various properties such as surface roughness, temperature, and thickness [4]. Consequently, in this work, scattering parameter measurements (S-parameter) are conducted on different material samples of traffic objects which can be commonly found in traffic scenarios. The measurement results are studied on the reflectivity and scattering behavior of the material. Furthermore, the measured S-parameters can be post-processed to determine the dielectric parameters of the utilized material to assign the corresponding values to the materials in traffic scenario simulations. The measurements in this work are conducted using the free-space method, which is a non-destructive dielectric characterization test method and applicable in a wide range of mm-wave frequencies like $76\,\mathrm{GHz}$ to $81\,\mathrm{GHz}$. The S-parameters of the material under test (MUT) are measured at different scanning angles to analyze its reflectivity behavior in automotive radar applications.

In this context, the fundamental of the measurement setup is discussed in Section II. Furthermore, it describes the measurement setup. Section III presents the reflection patterns of the sample under test. The data is further investigated to analyze the influence of different factors, such as scanning angles and surface roughness, on the reflection behavior of the materials. Moreover, the calculated relative permittivity from the measured data is discussed in Section III. Lastly, Section IV concludes the work by preparing a database of the measured traffic material properties and gives an outlook toward possible integration into the ASAM OpenMaterial database. In combination with some important additional data, this makes a simulation of traffic scenarios more realistic and comparable with other theoretical simulations.

II. Measurement Setup

There are various measurement methods to characterize the dielectric properties of materials, such as cavity resonators, wave-guides, and open-ended coaxial-probe methods. These methods can generally be classified into resonant and non-resonant techniques [5]. Non-resonant techniques are typically applied to obtain a general understanding of the material properties over a specific frequency range, despite possessing a lower degree of accuracy than the resonant methods. In these techniques, material properties can be

This work was supported by the German Federal Ministry of Education and Research (BMBF) through the VIVALDI Project under Grant 16ME0171.

derived based on the electromagnetic wave interaction with the material. Non-resonant methods principally use a coaxial line, waveguide, transmission line, or a highly directive antenna in a free-space setup. Among these techniques, the free-space method is a non-contact method that can be used for non-destructive testing of the samples since no mechanical machining of the samples is required as long as they are evenly flat. The free-space method can be used over a wide frequency range and under different conditions, e.g., temperature and humidity, and therefore is well-suited for automotive radar applications [5], [6].

The measurement setup of the free-space method, as shown in Fig. 1, is used to measure the S-parameters of the material sample, which is positioned between the transmitter (Tx) and receiver (Rx) antennas using a vector network analyzer (VNA).

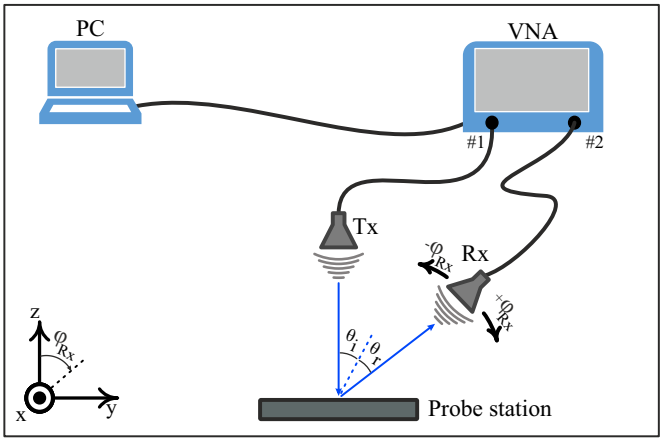

Fig. 1. Block diagram of measurement setup.

The measurement setup is equipped with an Agilent PNA-X VNA and Agilent mm-wave source extension module to collect the complex scattering parameters of MUT in the W-band. It has one degree of freedom to rotate the Rx antenna (φ_{Rx}) around the z-axis by utilizing a stepper motor. As shown in Fig. 2, the receiver antenna is mounted on a moving arm of the measurement setup to scan the MUT with a favorite angular step ($\Delta\varphi_{Rx}$).

The Tx and Rx antennas are horn antennas with a gain of 25 dBi. The half-power beam width (HPBW) of the antennas lies within $15.2°$ to $16.3°$ for a frequency range of 76 GHz to 81 GHz. The MUT should be placed on the far-field of the antennas so that the dominant part of the propagating wave can reach the sample with similar phases. The minimum far-field distance of the antennas for the configured frequency range is around 8.43 cm. Therefore, the probe station is fixed at least 35 cm away from the antennas to fulfill the far-field condition for all MUT. For measuring the S-parameters of the MUT, a sample of MUT is placed on the probe station and parallel to the xy-plane when the incident angle equals $0°$ and the transmitter is positioned above the center of the MUT. The scanning area for the Rx antenna is set to $\pm 50°$ with steps of $\Delta\varphi_{Rx} = 5°$. The specification of the measurement setup is summarized in Table I.

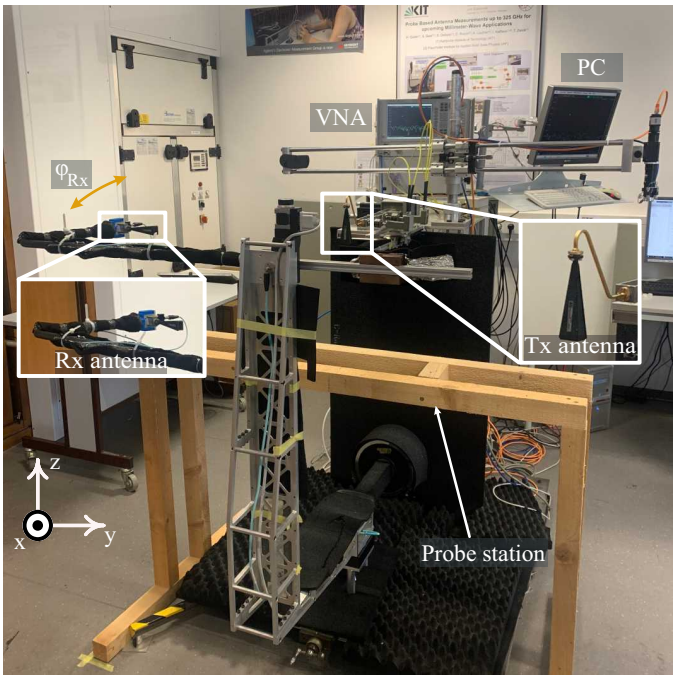

Fig. 2. Measurement setup to collect the S-parameters of MUT.

TABLE I
MEASUREMENT SETUP SPECIFICATION

Parameter	Setup Specification
Bandwidth (BW)	5 GHz
Starting frequency (f_{start})	76 GHz
Frequency step width (Δf)	5 MHz
Scanning angle (φ_{Rx})	$-50°$:$5°$:$50°$
Incident angle	$0°$

A three-step calibration is necessary to determine the resulting S-Parameters of the MUT. Firstly, the measurement setup is covered by mm-wave absorbers to reduce unwanted reflections from any component in the scanning area of the Rx antenna. Then, the systematic error of the free-space measurement method is compensated by the Thru-Reflect-Line (TRL) calibration method of VNA. In another calibration step, the test environment is characterized by measuring the probe station reflection pattern without any sample. After measuring the MUT, the S-parameters of the MUT can be determined using the mentioned calibration steps. Then, it is explained in Section III in more detail.

III. Measurement Results

The reflection behavior of some typical non-magnetic construction materials ($\mu_r = 1$) is analyzed in this work.

The list of the measured materials is given in Table II. The measured S-parameters (S_{21}) will be used to iteratively calculate the relative permittivity using Muller's method [7]. Fig. 3 shows some samples of the materials which are investigated in this work.

TABLE II
LIST OF MEASURED MATERIALS AND THEIR ESTIMATED RELATIVE PERMITTIVITY

MUT	Dimensions	Measured ε_r		Comments
	cm × cm × cm	$\varepsilon_r{}'$	$\varepsilon_r{}''$	
Asphalt ($AC8DS$)	30×26.5×4	4.44	0.38	Used on streets
Asphalt ($PA8$)	30×26.5×4	2.53	0.73	Used on highway for noise reduction
Concrete	40 × 40 × 4	4.71	0.26	-
Wood	30 × 30 × 3	2.07	0.15	-
Radome	22×13×2.3	2.5	0.024	-
Bumper	55×22×0.4	2.74	0.047	-

Fig. 3. Some samples of the measured materials.

The measured S-parameters for the MUT (S_{ij}^{MUT} where $i, j = 1\ or\ 2$) might be affected by multipath propagation, undesired reflections, and other interference. To reduce the impact of the measurement setup itself or any other relevant influences, a reference measurement is conducted to scan the measurement area in the absence of MUT (S_{ij}^{empty}). The S-parameters, which accurately reveal the scattering and reflectivity behavior of MUT, are calculated by

$$S_{ij,cal}^{MUT} = S_{ij}^{MUT} - S_{ij}^{empty}. \quad (1)$$

Then, the second reference measurement is conducted to collect the S-Parameters of a steel plate (S_{ij}^{STL}) as a reference material with an ideal smooth surface where specular reflection takes place. The used steel plate in the reference measurement possesses the same dimension as its corresponding MUT. In this situation, the amplitude of the measured S-parameters of the MUT (S_{ij}^{MUT}) can be normalized to the maximum measured amplitude for S-parameters of steel plate. The normalized amplitude of the measured S-parameters for the MUT can be written as

$$\left|S_{ij}^{MUT}\right|_{norm} = \frac{\left|S_{ij,cal}^{MUT}\right|}{max(\left|S_{ij}^{STL}\right|)}. \quad (2)$$

However, it should be noted that in this measurement setup, for the determination of the reflection parameters of the MUT, only the transmission parameters between the transmitting and the receiving antenna S_{21} are evaluated.

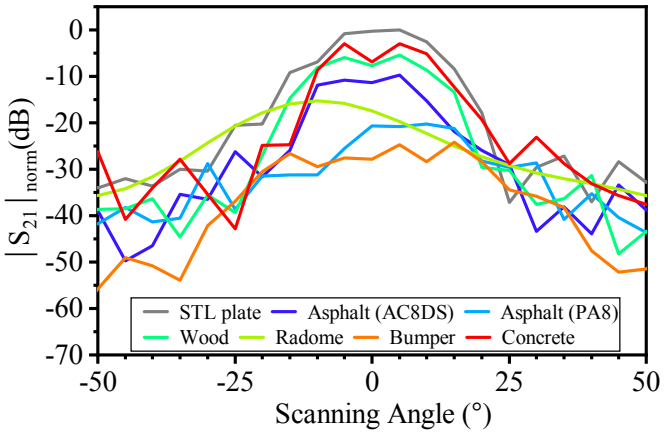

Fig. 4. Measured reflectivity pattern ($\left|S_{21}^{MUT}\right|_{norm}$) of different traffic materials in fixed incident angle of 0°.

A. Reflectivity Pattern of the Measured Samples at Fixed Incident Angle

The normalized amplitude of the measured S_{21} for the MUT is evaluated to determine its radar reflectivity behavior. Therefore, the measured $\left|S_{21}^{MUT}\right|_{norm}$ of the investigated samples are plotted in Fig. 4. It shows the radar reflectivity of the different samples at the fixed incident angle of 0° over different scanning angles. The physical dimensions ($L \times W \times H$) of the prepared samples for the measurement in this work are reported in Table II based on their length (L), width (W), and height (H).

By comparing the reflectivity of different measured materials, as it is expected, the steel plate has the highest reflectivity since it is an almost perfect conductor and its surface roughness is very small. Then, the concrete has more reflectivity behavior than asphalt samples, and it can be observed that the reflectivity behavior of the two asphalt samples is different.

It can be noticed, from the plots, that even though some of the materials possessed a certain degree of surface roughness, the dominant part of all of the reflected waves was focused towards the specular direction, showing the measurement setup is calibrated well. Indeed, that enables the comparison of the reflection coefficient of different materials. Moreover, it is also observed that the difference in reflectivity of two different types of asphalt samples is approximately $15\,\mathrm{dB}$. This shows that the reflection behavior of different kinds of asphalts is not identical, especially the asphalt sample of type AC8DS has a smoother surface than type PA8. This information is useful in modeling the test environment of the real traffic scenarios simulations.

The material quality of bumpers and radomes significantly influences the performance of automotive radar sensors considering that they are usually mounted behind bumpers or radomes. Therefore, studying their reflection patterns is a topic of interest in modeling mounting and material effects. Moreover, any angular errors, signal distortions, and attenuation can be analyzed and modeled to approach a more realistic wave propagation simulation. Therefore, two samples of a car bumper and radome are measured. The reflectivity pattern of the measured radome shows that it has roughly $-15\,\mathrm{dB}$ less reflectivity than the measured reference steel plate, and the reflection angle is shifted by $10°$ due to some curvature from the structures of the measured sample radome. However, the radomes are designed not to attenuate or disrupt the radar signal; such a flawless radome can never be achieved because of some requirements in other operational functionalities. Considering the $\left|\mathrm{S}_{21}^{MUT}\right|_{norm}$ plot of the bumper sample, it can be noticed that the bumper has a low reflectivity behavior and its degradation on radar signal quality is negligible. Concisely, different materials can be distinguished by their respective $\left|\mathrm{S}_{21}^{MUT}\right|_{norm}$ plots, as the reflection behavior of every material sample is unique.

The measurement setup is configured with $5\,\mathrm{GHz}$ bandwidth around the center frequency of $78.5\,\mathrm{GHz}$ with a frequency step of $5\,\mathrm{MHz}$. The collected measurement data is utilized to examine the reflectivity behavior of different samples at different frequencies. Fig. 5 shows the measured $\left|\mathrm{S}_{21}^{MUT}\right|_{norm}$ of different samples over the frequency with an incident angle of $0°$ and scanning angle of $-10°$. Although different scanning angles of the samples have been measured and investigated; for the sake of clarity, only the results of scanning angle $-10°$ is discussed here, and other results will be available in [8]. Additionally, the resonance frequency of measured materials can be investigated at a fixed incident angle and different scanning angles. For example, the concrete sample plot, for the mentioned incident and scanning angles shows two resonance

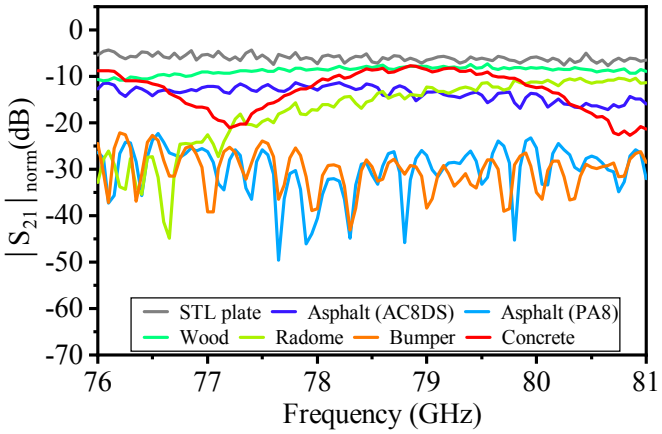

Fig. 5. Measured $\left|\mathrm{S}_{21}^{MUT}\right|_{norm}$ of different traffic materials over frequency in fixed incident angle of $0°$ and scanning angle of $\varphi_{Rx} = -10°$.

frequencies at $77.2\,\mathrm{GHz}$ and $80.75\,\mathrm{GHz}$.

The relative permittivity (ε_r) of a material can be derived from its scattering parameters. In this work, the Muller's method [9] is used, which is an iterative method, to calculate the complex relative permittivity ($\varepsilon_r = \varepsilon_r' - \mathrm{j}\varepsilon_r''$) of the measured non-magnetic material samples. The calculated values are listed in Table II.

For validation purposes, the measured relative permittivity for some of the materials is compared with the reported values for similar materials in the literature. For example, [10] and [11] report $\varepsilon_r' = 2.52$ and 4.46 for a similar measured asphalt and concrete sample in $77\,\mathrm{GHz}$, respectively. [12] approximates a relative permittivity of $\varepsilon_r = 1.57 - j0.06$ for a wood sample in $60.2\,\mathrm{GHz}$. The comparison of the measured values in this work and reported values in the literature shows a good agreement. It is shown in [11], [13] that the relative permittivity of environmental materials in the configured frequency range ($76\,\mathrm{GHz}$-$81\,\mathrm{GHz}$) is roughly constant.

The measured scattering parameters and calculated relative permittivity for the studied materials in this work are prepared in ASAM OpenMaterial format [14] and reported in [8]. The complex relative permittivity is a function of the dielectric properties which can be influenced by the physical properties of the sample, e.g., surface roughness, size, and humidity level. Moreover, the test environmental specifications, e.g., temperature, and humidity, have an influence on the measured scattering parameters and, consequently, estimated relative permittivity. Therefore, the physical properties of the sample, the test environment specification, the measurement method, and the utilized method for calculating the complex relative permittivity are reported in the ASAM OpenMaterial format.

IV. Conclusion

In this work, the scattering parameters of typical construction materials relevant to the simulations of radar wave propagation in traffic scenarios are measured. The measurement setup is based on the free-space method, and

the required reference measurements are explained in detail, which removes possible systematic errors in the setup. The reflectivity behavior of the measured samples is analyzed, and their complex relative permittivity is derived based on an iterative algorithm (Muller's method). The measured data is further processed to prepare a material properties look-up table in the format of ASAM OpenMaterial. This is important for the virtual development of autonomous driving systems and physical sensor simulations. Besides sensor simulation, modern rendering solutions also require physical material properties in 3D models in order to be able to reproduce physically correct reflections and shadowing. Thus, implementing physical correctness, like modeling material properties, in traffic scenario simulations can help to achieve valid results during the wave propagating simulations.

REFERENCES

[1] S. Riedmaier, J. Nesensohn, C. Gutenkunst, B. Schick, T. Düser, and H. Abdellatif, "Validation of x-in-the-loop approaches for virtual homologation of automated driving functions," in *11th Graz Symposium Virtual Vehicle (GSVF)*, 2018.

[2] A. Ngo, M. P. Bauer, and M. Resch, "A multi-layered approach for measuring the simulation-to-reality gap of radar perception for autonomous driving," in *2021 IEEE International Intelligent Transportation Systems Conference (ITSC)*, 2021, pp. 4008–4014.

[3] O. Landron, M. Feuerstein, and T. Rappaport, "A comparison of theoretical and empirical reflection coefficients for typical exterior wall surfaces in a mobile radio environment," *IEEE Transactions on Antennas and Propagation*, vol. 44, no. 3, pp. 341–351, 1996.

[4] B. Langen, G. Lober, and W. Herzig, "Reflection and transmission behaviour of building materials at 60 ghz," in *5th IEEE International Symposium on Personal, Indoor and Mobile Radio Communications, Wireless Networks - Catching the Mobile Future.*, vol. 2, 1994, pp. 505–509 vol.2.

[5] L. Chen, C. Ong, C. Neo, V. Varadan, and V. Varadan, *Microwave electronics*. Hoboken, NJ: Wiley-Blackwell, Mar. 2004.

[6] M. Kaniecki, E. Saenz, L. Rolo, R. Appleby, and O. Breinbjerg, "Scattering-parameter extraction and calibration techniques for rf free-space material characterization," in *The 8th European Conference on Antennas and Propagation (EuCAP 2014)*, 2014, pp. 1093–1097.

[7] D. Ghodgaonkar, V. Varadan, and V. Varadan, "A free-space method for measurement of dielectric constants and loss tangents at microwave frequencies," *IEEE Transactions on Instrumentation and Measurement*, vol. 38, no. 3, pp. 789–793, 1989.

[8] "Asam openmaterial." [Online]. Available: https://github.com/SevdaKIT1234/KIT-radar-reflectivity-Meas./tree/Sevda-Abadpour-(KIT)

[9] William H. Press, B. P. Flannery, S. A. Teukolsky, and W. T. Vetterling, *Numerical recipes in FORTRAN 77: Volume 1 of FORTRAN numerical recipes volume 1*, 2nd ed. Cambridge, England: Cambridge University Press, Sep. 1992.

[10] V. Kurz, H. Stuelzebach, F. Pfeiffer, C. van Driesten, and E. Biebl, "Road surface characteristics for the automotive 77 ghz band," *Advances in Radio Science*, vol. 19, pp. 165–172, 2021. [Online]. Available: https://ars.copernicus.org/articles/19/165/2021/

[11] S. S. Zhekov, O. Franek, and G. F. Pedersen, "Dielectric properties of common building materials for ultrawideband propagation studies [measurements corner]," *IEEE Antennas and Propagation Magazine*, vol. 62, pp. 72–81, 2020.

[12] Y. Shao, X. Liao, and Y. Wang, "Complex permittivity of typical construction materials over 40–50 ghz," in *2018 IEEE International Symposium on Antennas and Propagation USNC/URSI National Radio Science Meeting*, 2018, pp. 2003–2004.

[13] D. McGraw, "The measurement of the dielectric constant of concrete pipes and clay pipes," Ph.D. dissertation, College of Engineering & Science, Louisiana Tech University, 2013.

[14] "Asam openx standards." [Online]. Available: https://www.asam.net/standards/